

# **NT\*-HRV3CP: an optimized construct of human rhinovirus 14 3C protease for high-yield expression and fast affinity-tag cleavage**

Elwy H. Abdelkader and Gottfried Otting\*

ARC Centre of Excellence in Innovations in Peptide and Protein Science, Australian National University, Research School of Chemistry, Canberra, ACT 2601, Australia

\* Corresponding author

E-mail address: gottfried.otting@anu.edu.au

## Abstract

The human rhinovirus 14 3C protease (HRV3C protease), in fusion with glutathione S-transferase also referred to as PreScission™ protease, is a cysteine protease of particular interest for affinity tag removal from fusion proteins due to its stringent recognition sequence specificity (LEVLFQ/GX) and superior activity at low temperature. Here we report the expression, purification and use of a fusion construct of HRV3C protease, NT\*-HRV3CP, that affords high expression yield in *E. coli* (over 300 mg/L cell culture), facile single-step purification, high solubility (>10 mg/mL) and excellent storage properties. NT\*-HRV3CP cleaves affinity tags at 4 °C in minutes, making it an attractive tool for the production of recombinant proteins for biotechnological, industrial and pharmaceutical applications.

Keywords: human rhinovirus 14 3C protease; PreScission protease; NT\* fusion protein; fusion tag cleavage

## Introduction

Fusion tags have become indispensable tools for affinity purification and solubility enhancement of recombinant proteins. Affinity tags such as polyhistidine, glutathione S-transferase (GST) or chitin binding domains (CBD) facilitate the selective purification of the target proteins, whereas maltose binding protein (MBP) and GST are widely used to enhance their solubility (Kimple et al., 2013; Lichty et al., 2005). Fusion tags have also successfully been used to protect their fusion partners from proteolytic degradation and promote their proper folding during expression, improving the yield of active proteins (Costa et al., 2014; Malik, 2016; Raran-Kurussi and Waugh, 2012).

To recover the native activities of the protein of interest, the fusion tags need to be removed after purification of the fusion construct. This is commonly achieved by inserting a specific polypeptide sequence between the fusion tag and its fusion partner, which is recognized by a specific proteolytic enzyme (Waugh, 2011). The most widely used enzymes for fusion tags removal are endoproteases, including serine proteases such as thrombin (Plavša et al., 2018), enterokinase (Huang et al., 2007) and cysteine proteases such as tobacco etch virus (TEV) protease (Yi et al., 2013) and human rhinovirus 14 3C (HRV 3C) protease (Ullah et al.,

2016). The stringent specificity of the viral cysteine proteases makes them the enzymes of choice for endoproteolytic removal of affinity tags over serine proteases (Waugh, 2011).

The HRV 3C protease, the GST fusion of which is also known as PreScission™ protease (Leong, 1999), is a 20 kDa cysteine protease derived from human rhinovirus type 14, which cleaves specifically between the glutamine and glycine residues of the recognition sequence LEVLFQ/GP. The HRV 3C protease is highly active even at 4 °C, making it the protease of choice for the processing of temperature-sensitive recombinant proteins (Raran-Kurussi et al., 2013; Ullah et al., 2016). A recent analysis of the substrate specificity of HRV 3C protease showed that the specificity for a proline residue in the P2' position of the recognition site is more relaxed than commonly assumed. In fact, the authors suggested LEVLFQ/GM as an even better recognition sequence and showed that any of the other canonical amino acids can also be tolerated in the P2' position, albeit leading to reduced cleavage efficiency (Fan et al., 2020). The somewhat relaxed specificity for the residue in the P2' site and its much greater activity at 4 °C compared with the TEV protease render the HRV 3C protease an attractive tool for cleaving affinity tags.

Unfortunately, the production of HRV 3C protease in *E. coli* is not straightforward as the protease is prone to forming inclusion bodies when over-expressed (Birch et al., 1995; Xu et al., 2019). This complicates its purification, requiring a lengthy refolding protocol in order to obtain active enzyme (Birch et al., 1995). Only limited literature is available on alternative expression protocols of the HRV C3 protease. GST (Antoniou et al., 2017) and the biotin acceptor peptide (BAP) (Youell et al., 2011) have been proposed and shown to enhance the production of soluble HRV 3C protease. Yields of 22 mg/L and 25-30 mg/L cell culture were reported for HRV 3C protease tagged with GST or BAP, respectively. Expression constructs in fusion with mutant DsbA (Zhang et al., 1998) and His<sub>6</sub> and MBP tags (Walker et al., 1994) have also been made, but protein yields were not reported.

Here we report a new fusion construct for recombinant HRV 3C protease (NT\*-HRV3CP) which delivers exceptional expression yield, solubility and proteolytic activity at 4 °C. The fusion is based on the N-terminal domain of the spider silk protein NT\*, which has previously been shown to confer excellent solubility enhancement on fusion partners (Abelein et al., 2020; Kronqvist et al., 2017).

## 1. Materials and methods

### 1.1. Design and molecular cloning

The new recombinant fusion of HRV 3C protease, NT\*-HRV3CP, comprises an N-terminal His<sub>6</sub> tag following by the amino acid sequence of the NT\* domain (Kronqvist et al., 2017), a flexible Ser-Gly<sub>4</sub>-Ser linker and the HRV 14 3C protease (NCBI accession No. **NP\_740524.1**).

The proteolytic activity of NT\*-HRV3CP was tested with a construct of N-terminally His<sub>6</sub>-tagged red fluorescent protein (his-RFP) with the HRV 3C protease recognition site inserted between the His<sub>6</sub> tag and the RFP sequence (NCBI accession No. **AEA29852**). The amino acid sequences of the final NT\*-HRV3CP and his-RFP constructs are shown in Fig. 1.

The DNA sequences encoding NT\*-HRV3CP and his-RFP were synthesized by Integrated DNA Technologies (USA). NT\*-HRV3CP and his-RFP genes were cloned between *NdeI* and *BamHI* restriction sites of pET-47b(+) and pET-3a plasmids (Novagen, USA), respectively, using *E. coli* DH10B cells with a previously published cloning protocol (Qi and Otting, 2019). The expression plasmid for NT\*-HRV3CP has been submitted to Addgene, (Teddington, UK) (plasmid # 162795)

(a)

***MHHHHH***SHTTPWTNPGLAENFMNSFMQGLSSMPGFTASQLDKMSTIAQSMVQS  
*IQSLAAQGR*TSPNDLQALNMAFASSMAEIAASEEGGSLSTKTSSIASAMSNF  
LQTTGVVNQPFINEITQLVSMFAQAGMNDVSAGNSGGGSGPNTEFALSLLRKN  
IMTITTSKGEFTGLGIHDRVCVIPTHAQPGDDVLVNGQKIRVKDKYKLVDPENI  
NLELTVLTLDRNEKFRDIRGFISEDLGVDATLVVHSNNFTNTILEVGPVTMAG  
LNLSSPTNRMIRYDYATKTGQCGVLCATGKIFGIHVGGNGRQGFSAQLKKQ  
YFVEKQ

(b)

***MHHHHH***LEVLFQGPASSEDVIKEFMRFKVRMEGSVNGHEFEIEGEGEGRPYEG  
TQTAKLKVTKGGPLPFAWDILSPQFQYGSKAYVKHPADIPDYLLKLSFPEGFKWE  
RVMNFEDGGVVTVTQDSSLQDGEFIYKVKLRGTNFPDGPVMQKKTMGWEASTE  
RMYPEDGALKGEIKMRLKLDGGHYDAEVKTTYMAKKPVQLPGAYKTDIKLDIT  
SHNEDYTIVEQYERAEGRHSTGA

**Fig. 1.** Full amino acid sequences of the constructs used in the present work. **(a)** Amino acid sequence of NT\*-HRV3CP. The sequences of the His<sub>6</sub> tag and Ser-Gly<sub>4</sub>-Ser linker are highlighted in bold and italics, respectively. The sequence of the NT\* solubility tag is underlined and the sequence of the HRV 3C protease is identified by double underlining. **(b)** Amino acid sequence of his-RFP. The sequence of the His<sub>6</sub> tag is highlighted in bold and the HRV 3C protease recognition site is underlined.

## 1.2. Protein expression and purification

All proteins were expressed *in vivo* in *E. coli* BL21(DE3) cells (Invitrogen, USA). To produce NT\*-HRV3CP, the pET-47b(+) plasmid was transformed into *E. coli* BL21(DE3) cells and the cells were grown at 37 °C in Luria–Bertani (LB) medium containing 50 µg/L kanamycin. An aliquot (2.5 mL) of an overnight culture was used to inoculate 250 mL terrific broth (TB) medium supplemented with 50 µg/L kanamycin. The cells were grown at 37 °C to an OD<sub>600</sub> of 0.6–1. Next, the temperature was reduced to 18 °C and protein expression induced by adding 0.5 mM isopropyl-β-D-thiogalactopyranoside (IPTG). To produce his-RFP, the pET-3a plasmid was transformed into *E. coli* BL21(DE3) cells and the cells were grown at 37 °C in LB medium containing 100 µg/L ampicillin. An aliquot (10 mL) of an overnight culture was used to inoculate 1 L LB medium supplemented with 100 µg/L ampicillin. The cells were grown at 37 °C to an OD<sub>600</sub> of 0.6–1. At this point the temperature was reduced to 25 °C and protein expression induced by adding 1 mM IPTG.

After expression for 16 h, the cells were harvested by centrifugation and resuspended in buffer A (50 mM Tris-HCl pH 7.5, 300 mM NaCl, 5% glycerol, 10 mM imidazole) followed by lysis using an Avestin Emulsiflex C5 (Avestin, Canada) (two passes using 10,000–15,000 psi). The cell lysates were centrifuged for 1 h at 30,000 g. The supernatant was loaded onto a 5 mL HisTrap FF column connected to an ÄKTA pure 25 chromatography system (Cytiva, USA). The column was washed with 20 column volumes buffer B (same as buffer A but with 20 mM imidazole) and then the protein was eluted with 3 column volumes buffer C (same as buffer A but with 500 mM imidazole). The eluted protein was desalted using a HiPrep Desalting 26/10 column (Cytiva, USA) equilibrated with buffer D (50 mM Tris-HCl buffer pH 7.5, 300 mM sodium chloride, 1 mM dithiothreitol (DTT)). Afterwards, the proteins were concentrated using an Amicon ultrafiltration centrifugal tube (Merck Millipore, USA) with a molecular weight cut-off of 10 kDa. NT\*-HRV3CP was stored in 10% glycerol at -80 °C after snap freezing in liquid nitrogen, while his-RFP was stored at -20 °C. Protein concentrations were measured with a NanoDrop One<sup>C</sup> spectrophotometer (NanoDrop Technologies, USA) using the 280 nm extinction coefficients of 11460 and 32890 M<sup>-1</sup> cm<sup>-1</sup> calculated for NT\*-HRV3CP and his-RFP, respectively (Gasteiger et al., 2005).

Size-exclusion chromatography (SEC) was performed on an ÄKTA pure 25 chromatography system using a HiLoad 26/600 Superdex 200 pg 120 mL column (Cytiva, USA) equilibrated with buffer E (50 mM Tris-HCl pH 7.5, 400 mM sodium chloride, 1 mM DTT) at a flow rate of 1 mL/min.

Circular Dichroism (CD) was performed on a Chirascan<sup>TM</sup> spectrometer (Applied Photonics, UK) with 0.1 cm path length quartz cuvette at 220 nm. 400 µL samples of NT\*-HRV3CP were prepared using 50 mM sodium phosphate buffer, pH 7.5, at a protein concentration of 0.2–0.3 mg/mL.

The on-column tag cleavage experiment was conducted with clarified lysate from a 100 mL cell culture of *E. coli* BL21(DE3) cells expressing his-RFP. Following loading onto a 1 mL His GraviTrap column (Cytiva, USA) pre-equilibrated with buffer A, the column was washed with 20 column volumes of buffer B containing 1 mM DTT and 1 mL of 10 µM NT\*-HRV3CP was loaded onto the column. After incubating the column at 4 °C for 3 h, 5 column volumes of buffer B were added to collect the cleaved his-RFP. Finally, 5 column volumes of buffer C were added to elute any un-cleaved his-RFP and NT\*-HRV3CP.

### 1.3. NT\*-HRV3CP activity test

To samples of 20 µM his-RFP in buffer D incubated on ice, NT\*-HRV3CP was added to a final concentration of 20, 2, 0.2 or 0.02 µM. The samples were stirred at the specified temperature and progress of the proteolytic cleavage was monitored by intact protein mass spectrometry, taking 20 µL aliquots from each reaction at different times (up to 16 h) and quenching the reaction by adding formic acid to 0.1% final concentration. Samples were loaded onto 1 mL His GraviTrap columns (Cytiva, USA) pre-equilibrated with buffer A. The columns were washed with 5 column volumes buffer A and eluted with 5 column volumes buffer C. Protein samples were analysed by SDS-PAGE using NuPAGE 4–12% Bis-Tris gels (Thermo Fisher Scientific, USA).

To determine the percentage of RFP recovered after Ni-NTA column purification, the RFP fluorescence was analysed at 25 °C on a SpectraMax microplate reader (Molecular Devices, USA) at 582 nm excitation wavelength and 640 nm emission wavelength.

#### 1.4. Intact protein mass spectrometry

Intact protein analysis was performed on an Orbitrap Fusion Tribrid mass spectrometer (Thermo Fisher Scientific, USA) connected to a Thermo Fisher Scientific UltiMate 3000 HPLC system equipped with ZORBAX 300SB-C3, 3.5 µm, 4.6 x 50 mm HPLC column (Agilent Technologies, USA). Each HPLC run consisted of a 500 µL/min linear gradient of solvent A (0.1% (v/v) formic acid in water) and solvent B (0.1% (v/v) formic acid in acetonitrile), ramping solvent B from 5% solvent B at the start to 80% after 12 min. Data were collected using an electrospray ionization (ESI) source in positive ion mode. Protein intact mass was determined by deconvolution using the Xtract function in the Qual Browser software tool of the program Xcalibur 3.0.63 (Thermo Fisher Scientific, USA).

## 2. Results

### 2.1. Protein expression and purification

*E. coli* BL21(DE3) cells expressed our newly designed HRV3CP construct with N-terminal NT\* tag (NT\*-HRV3CP) in high yield and predominantly in the soluble fraction, as shown by SDS-PAGE analysis (Fig. 2a). A single affinity chromatography step using a Ni-NTA column yielded NT\*-HRV3CP with more than 95% purity as indicated by SEC analysis and intact protein mass spectrometry (Fig. 3). The yield of purified NT\*-HRV3CP was  $305 \pm 16$  mg/L cell culture (mean of three separate expression experiments  $\pm$  standard deviation) or about 44 mg/g wet cells. This yield exceeds the reported yield of HRV 3C protease tagged with GST or BAP more than 10-fold (Antoniou et al., 2017; Youell et al., 2011). In addition, NT\*-HRV3CP shows high solubility and can be concentrated to 10 mg/mL without aggregation or precipitation.

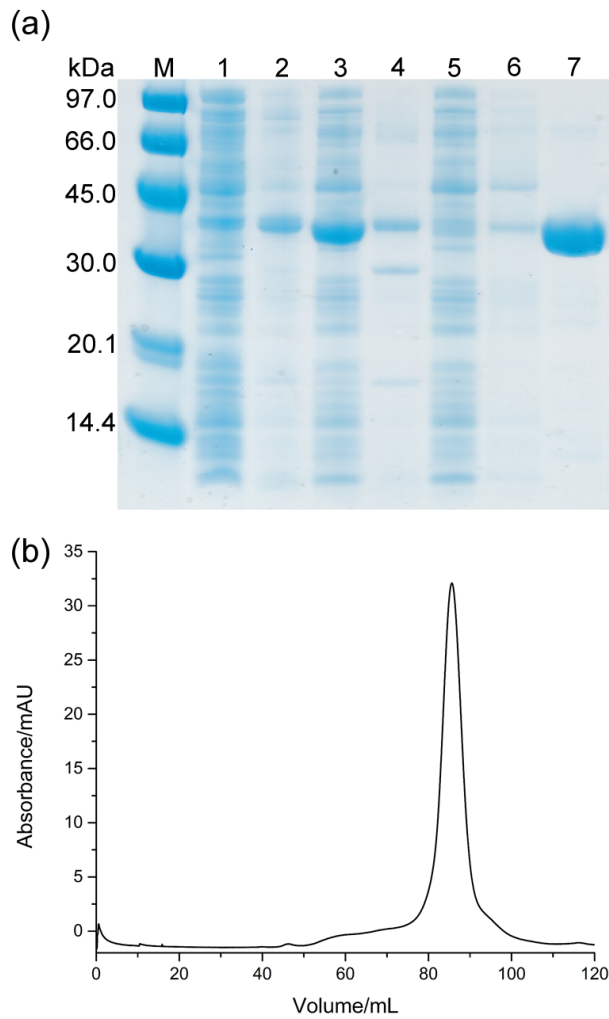


**Fig. 2.** NT\*-HRV3CP expression and purification. **(a)** SDS-PAGE analysis: M, protein molecular weight marker (the size of each band is indicated on the left); lane 1, lysate of BL21 cells before induction; lane 2, cell lysate 16 h after induction; lane 3, soluble fraction; lane 4, cell pellet after centrifugation; lane 5, flow-through from Ni-NTA column; lane 6, Ni-NTA column wash; lane 7, Ni-NTA column elution. **(b)** SEC analysis of purified NT\*-HRV3CP. The chromatogram shows a single peak at the elution time expected for monomeric NT\*-HRV3CP.

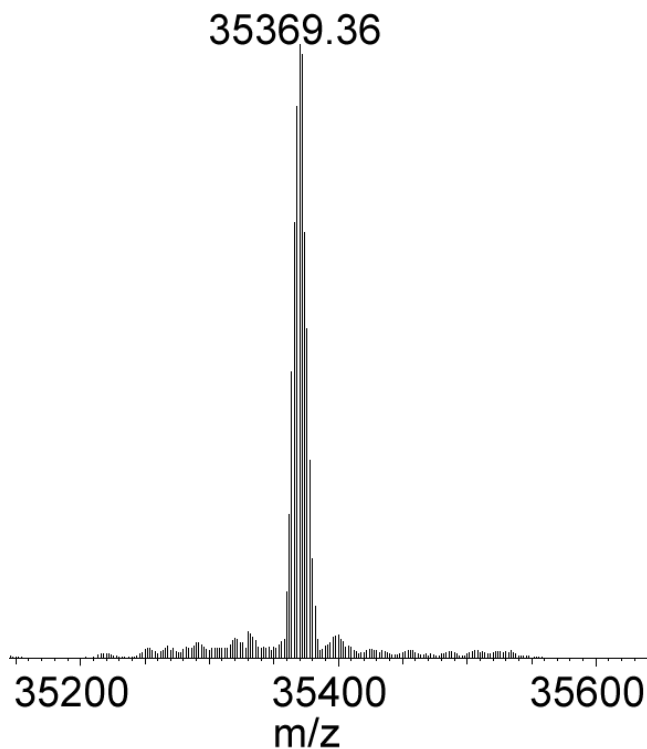


**Fig. 3.** Intact protein mass spectrum of NT\*-HRV3CP. The expected mass is 35,371.05 Da.

## 2.2. NT\*-HRV3CP proteolytic activity

The proteolytic activity of NT\*-HRV3CP was tested using an N-terminal His<sub>6</sub>-tagged RFP construct (his-RFP) with a HRV 3C protease cleavable site between the His<sub>6</sub> tag and RFP. his-RFP was incubated with NT\*-HRV3CP at 4 different molar ratios (1:1, 1:0.1, 1:0.01 and 1:0.001) and the progress of the proteolytic cleavage at 4 °C was monitored by intact protein mass spectrometry (Fig. 4 and 5). At equimolar ratio, 97% of his-RFP was cleaved after 15 minutes (Fig. 4b) and cleavage was complete after 1 h. At the molar ratio 1:0.1, 98% of his-RFP was cleaved after 1 h. At the molar ratio 1:0.01, 3 h were required to achieve 97% cleavage. At a molar ratio of 1:0.001, 87% cleavage was achieved after 16 h incubation.

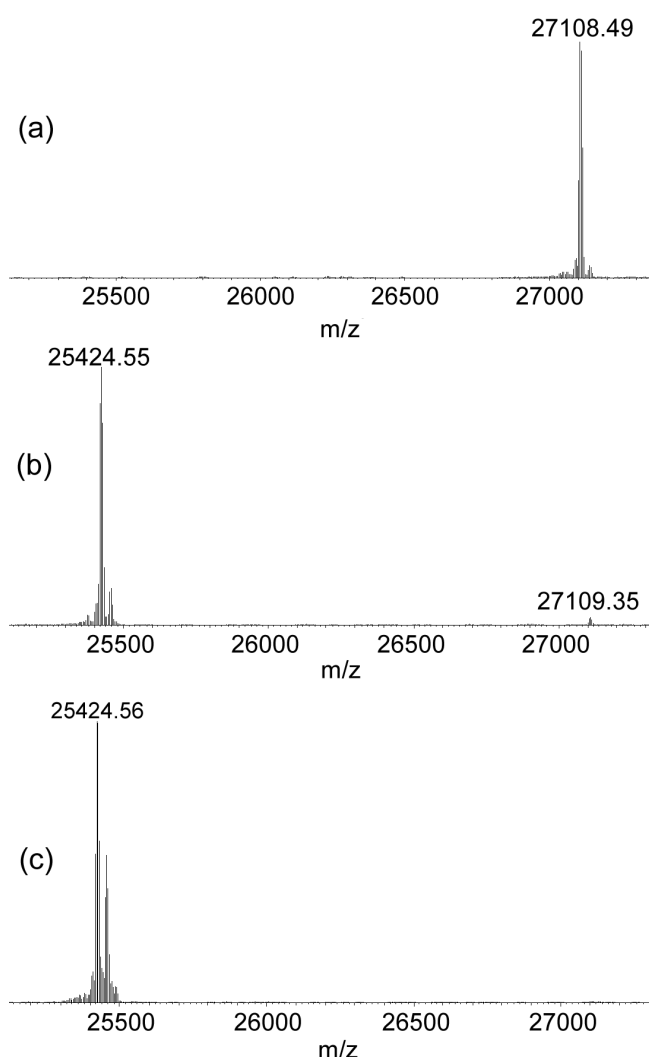


**Fig. 4.** Mass spectra of his-RFP before and after cleavage of the His<sub>6</sub> tag with NT\*-HRV3CP. **(a)** Before cleavage. The expected mass is 27108.61 Da. **(b)** After incubation with an equimolar amount of NT\*-HRV3CP (absolute concentration 20  $\mu$ M) at 4  $^{\circ}$ C for 15 minutes. The spectrum shows a minor peak at 27,109.35 Da corresponding to un-cleaved his-RFP while the main peak corresponds to cleaved his-RFP (expected mass 25,424.69 Da). **(c)** Same as (b), but after incubation with NT\*-HRV3CP for 16 h.

To test the effect of temperature on the activity of NT\*-HRV3CP, his-RFP was incubated with 0.01 equivalents NT\*-HRV3CP at 25 and 37  $^{\circ}$ C (Fig. 5b). At 25  $^{\circ}$ C, more than 90% of his-RFP was cleaved within 30 minutes and complete cleavage was achieved within 1 hour. At 37  $^{\circ}$ C, no significant increase in NT\*-HRV3CP activity was observed, suggesting that the maximum activity of NT\*-HRV3CP is achieved at 25  $^{\circ}$ C. These results show that the NT\* tag delivered highly soluble as well as active HRV 3C protease.



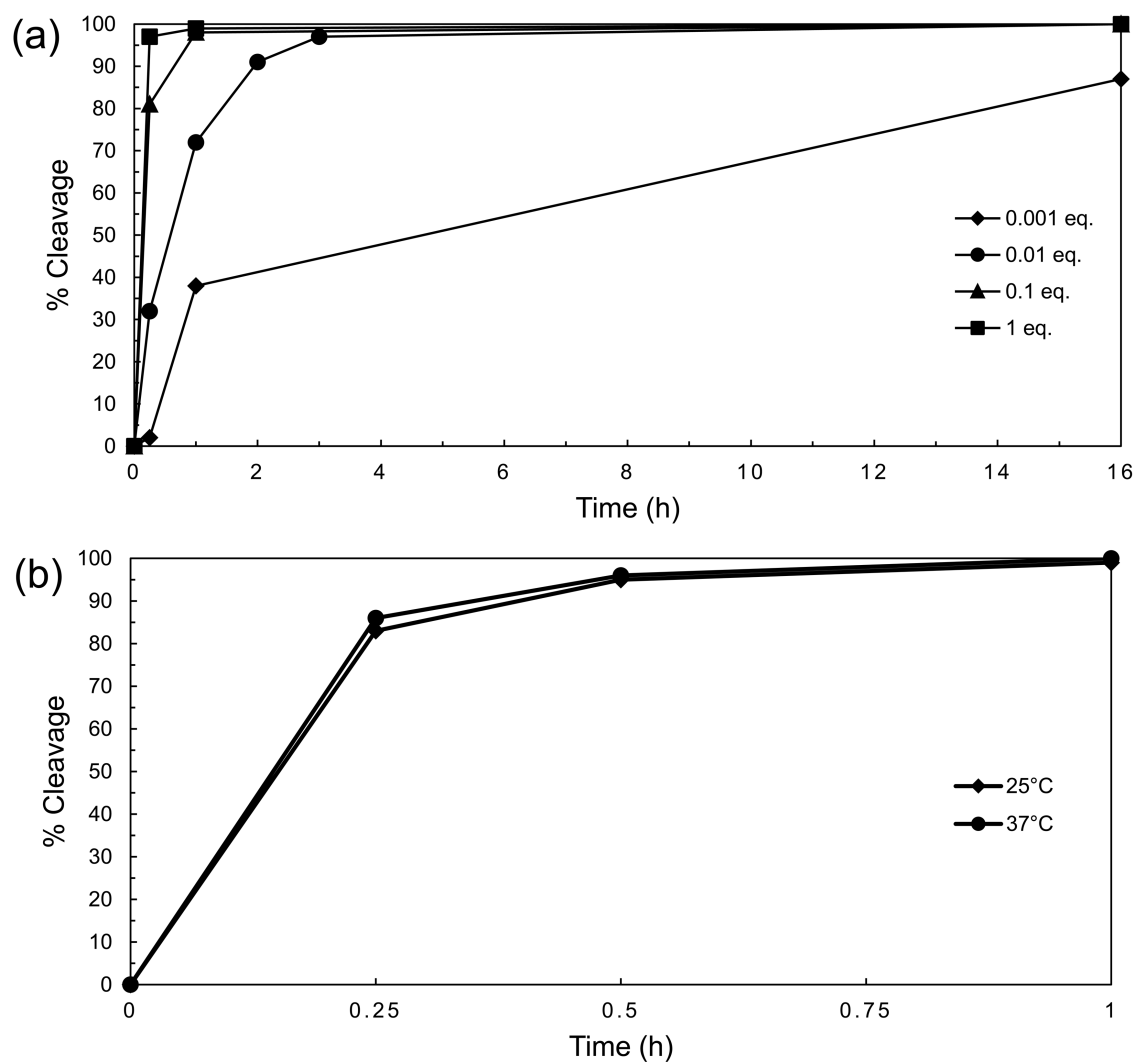


**Fig. 5.** NT\*-HRV3CP activity tests. **(a)** Progress of his-RFP cleavage at 4 °C at four different molar ratios. The percentage of successful cleavage was estimated from the relative peak heights of cleaved and un-cleaved his-RFP in intact protein mass spectra. **(b)** Progress of his-RFP cleavage at 0.01 equivalents of NT\*-HRV3CP at 25 and 37 °C.

To check for the occurrence of non-specific cleavage as a result of a high molar ratio of protease to target protein, his-RFP was subjected to 16 h incubation with an equimolar amount of NT\*-HRV3CP at 4 °C. No sign of non-specific cleavage or degradation was detected by mass spectrometry (Fig. 4c). As expected, Ni-NTA purification of the sample yielded RFP only in the flow-through fraction and no RFP fluorescence was detected in the elution fraction (Fig. 6). The recovery of RFP after this purification step was  $87 \pm 3$  % (mean of three separate purifications  $\pm$  standard deviation).

In addition, NT\*-HRV3CP was tested for its performance in on-column tag cleavage (Fig. 6). Following loading of crude clarified cell lysate containing his-RFP onto a His GraviTrap column, a wash step removed non-specifically bound proteins. Next, NT\*-HRV3CP was loaded onto the column and incubated for 3 hours at 4 °C. A second wash step collected cleaved his-RFP and un-cleaved his-RFP and NT\*-HRV3CP were collected in a final elution

step. The recovery of his-RFP following on-column tag removal was  $75 \pm 5$  % (mean of three separate purifications  $\pm$  standard deviation).

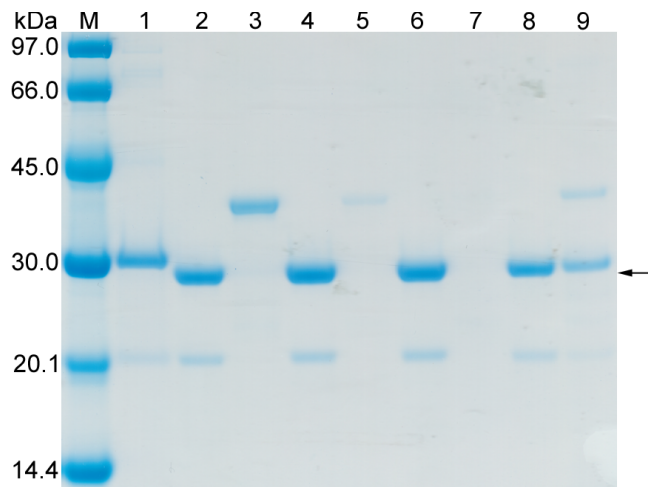


**Fig. 6.** SDS-PAGE analysis of the proteolytic activity of NT\*-HRV3CP. The arrow identifies the band of RFP following cleavage of the His<sub>6</sub> tag. M, protein molecular weight marker (the size of each band is indicated on the left); lane 1, his-RFP before cleavage; lanes 2 and 3, Ni-NTA flow-through and elution fractions of the cleavage reaction conducted with equimolar NT\*-HRV3CP for 16 h; lanes 4 and 5, same as lanes 2 and 3, but following incubation with 10 times less NT\*-HRV3CP; lanes 6 and 7, same as lanes 2 and 3, but following incubation with 100 times less NT\*-HRV3CP. Lanes 8 and 9 are the wash and elution fractions, respectively, illustrating the cleavage of his-RFP after on-column incubation with NT\*-HRV3CP for 3 hours at 4 °C.

Finally, the proteolytic activity of NT\*-HRV3CP was compared to commercially available HRV 3C protease, Pierce™ HRV3CP (Thermo Fisher Scientific, USA). 1 μg NT\*-HRV3CP showed similar activity as 1 unit of Pierce™ HRV3CP at 4 °C (Fig. 7).

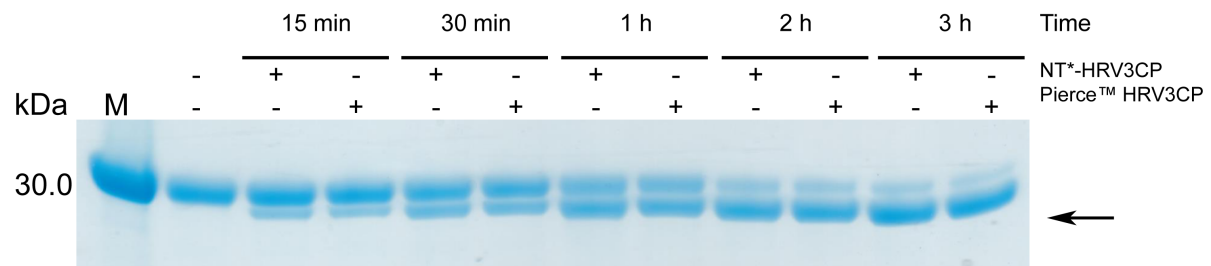


**Fig. 7.** Comparison between the proteolytic activity of NT\*-HRV3CP and Pierce™ HRV3CP at 4 °C, monitored by SDS-PAGE. The reactions were performed 20 μM his-RFP in 200 μL. M, molecular weight marker. The arrow marks the band of his-RFP following cleavage of the N-terminal His<sub>6</sub> tag.

Preparations of 10 mg/mL stock solutions of NT\*-HRV3CP in buffer D with 10% glycerol are stable at 4 °C for 2 weeks without precipitating, and no precipitation or decline in activity were observed following storage at -20 °C and several freeze-thaw cycles (Fig. 8).

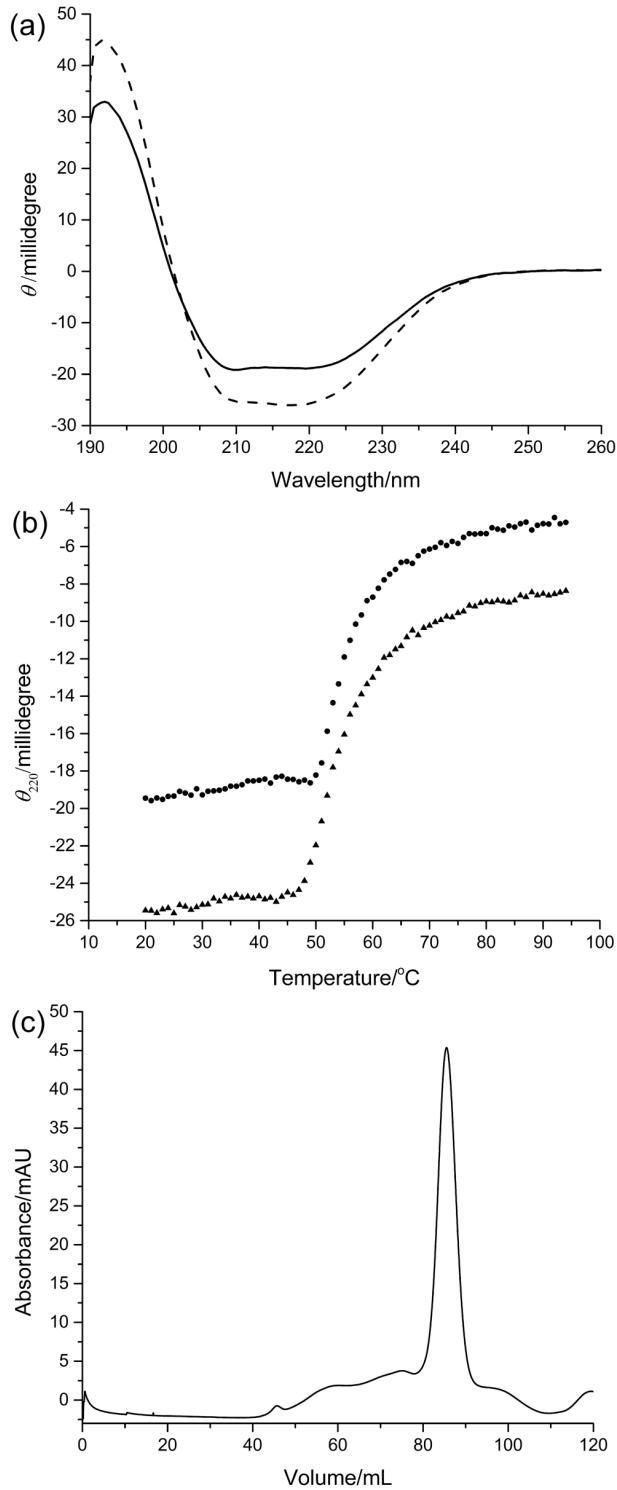


**Fig. 8.** Analysis of the thermal stability of NT\*-HRV3CP. **(a)** CD spectra of freshly expressed NT\*-HRV3CP (solid line) and after storage at -20 °C for 60 days (dashed line). The greater intensity of the sample recovered from storage reflects its somewhat greater

concentration (0.25 mg/mL versus 0.20 mg/mL). **(b)** Temperature denaturation of freshly expressed NT\*-HRV3CP (●) and following freezing at -20 °C and thawing (▲). The midpoints of the denaturation curves indicate similar melting temperatures ( $T_m$ ) of 55.7 and 54.6 °C, respectively. **(c)** SEC analysis of NT\*-HRV3CP following storage at 4 °C for 2 weeks, confirming the absence of significant aggregation or degradation.

### 3. Discussion

The ease with which highly active NT\*-HRV3CP can be obtained in high purity makes this construct an attractive tool for specific proteolytic cleavage. Compared with the widely used TEV protease, the HRV 3C protease is more active and tolerant to a wider range of commonly used buffer additives (Ullah et al., 2016). Typical cleavage conditions with TEV protease require incubation overnight when conducted at 4 °C. In contrast, NT\*-HRV3CP can achieve complete affinity tag removal in minutes at 4 °C. As the wild-type TEV protease displays limited stability towards aggregation and degradation, also the TEV protease has been subjected to mutation and modification for increased expression yields, solubility and activity in biotechnological applications (Cabrita et al., 2007; Tropea et al., 2009; Cesaratto et al., 2016; Mohammadian et al., 2020; Nam et al., 2020; Sanchez and Ting, 2020; Yi et al., 2013), usually without reporting activities at 4 °C. In our hands, the activity enhancing mutant S219V in the construct developed by Tropea et al. (2009) performs well but we never obtained expression yields exceeding 60 mg/L cell culture.

In conclusion, the NT\* fusion of the HRV 3C protease reported in the present work delivers high yields of a protease that has very desirable properties as a biotechnological tool but proved difficult to produce in larger quantities to date. The high expression yield of our fusion construct in *E. coli* combined with ease of purification, high solubility and intrinsically high specificity of proteolytic activity renders NT\*-HRV3CP an attractive tool for efficient affinity tag cleavage from fusion proteins in minutes.

### Acknowledgement

Financial support by the Australian Research Council for a Laureate Fellowship to G.O. (FL170100019) and through a Centre of Excellence (CE200100012) is gratefully acknowledged.

### References

- Abelein, A., Chen, G., Kitoka, K., Aleksis, R., Oleskovs, F., Sarr, M., Landreh, M., Pahnke, J., Nordling, K., Kronqvist, N., Jaudzems, K., Rising, A., Johansson, J., Biverstål, H., 2020. High-yield production of amyloid- $\beta$  peptide enabled by a customized spider silk domain. *Sci. Rep.* 10, 235. <https://doi.org/10.1038/s41598-019-57143-x>
- Antoniou, G., Papakyriacou, I., Papanephytous, C., 2017. Optimization of soluble expression and purification of recombinant human rhinovirus type-14 3C protease using statistically designed experiments: Isolation and characterization of the enzyme. *Mol. Biotechnol.* 59, 407–424. <https://doi.org/10.1007/s12033-017-0032-9>

Birch, G.M., Black, T., Malcolm, S.K., Lai, M.T., Zimmerman, R.E., Jaskunas, S.R., 1995. Purification of recombinant human rhinovirus 14 3C protease expressed in *Escherichia coli*. *Protein Expression Purif.* 6, 609–618. <https://doi.org/10.1006/pep.1995.1080>

Cabrita, L.D., Gilis, D., Robertson, A.L., Dehouck, Y., Rooman, M., Bottomley, S.P., 2007. Enhancing the stability and solubility of TEV protease using in silico design. *Protein Sci.* 16, 2360–2367. <https://doi.org/10.1110/ps.072822507>

Cesaratto, F., Burrone, O.R., Petris, G., 2016. Tobacco etch virus protease: a shortcut across biotechnologies. *J. Biotechnol.* 231, 239–249. <https://doi.org/10.1016/j.jbiotec.2016.06.012>

Costa, S., Almeida, A., Castro, A., Domingues, L., 2014. Fusion tags for protein solubility, purification and immunogenicity in *Escherichia coli*: the novel Fh8 system. *Front. Microbiol.* 5, 63. <https://doi.org/10.3389/fmicb.2014.00063>

Fan, X., Li, X., Zhou, Y., Mei, M., Liu, P., Zhao, J., Peng, W., Jiang, Z.-B., Yang, S., Iverson, B.L., Zhang, G., Yi, L., 2020. Quantitative analysis of the substrate specificity of human rhinovirus 3C protease and exploration of its substrate recognition mechanisms. *ACS Chem. Biol.* 15, 63–73. <https://doi.org/10.1021/acscchembio.9b00539>

Gasteiger, E., Hoogland, C., Gattiker, A., Duvaud, S.e., Wilkins, M.R., Appel, R.D., Bairoch, A., 2005. Protein identification and analysis tools on the ExpASY server. In: Walker, J.M. (Ed.), *The Proteomics Protocols Handbook*. Humana Press, Totowa, NJ, pp. 571–607. <https://doi.org/10.1385/1-59259-890-0:571>

Huang, L., Ruan, H., Gu, W., Xu, Z., Cen, P., Fan, L., 2007. Functional expression and purification of bovine enterokinase light chain in recombinant *Escherichia coli*. *Prep. Biochem. Biotechnol.* 37, 205–217. <https://doi.org/10.1080/10826060701386695>

Kimple, M.E., Brill, A.L., Pasker, R.L., 2013. Overview of affinity tags for protein purification. *Curr. Protoc. Protein Sci.* 73, 9.9.1–9.9.23. <https://doi.org/10.1002/0471140864.ps0909s73>

Kronqvist, N., Sarr, M., Lindqvist, A., Nordling, K., Otkovs, M., Venturi, L., Pioselli, B., Purhonen, P., Landreh, M., Biverstål, H., Toleikis, Z., Sjöberg, L., Robinson, C.V., Pelizzi, N., Jörnvall, H., Hebert, H., Jaudzems, K., Curstedt, T., Rising, A., Johansson, J., 2017. Efficient protein production inspired by how spiders make silk. *Nat. Commun.* 8, 15504. <https://doi.org/10.1038/ncomms15504>

Leong, L.E.C. (1999) The use of recombinant fusion proteases in the affinity purification of recombinant proteins. *Mol. Biotechnol.* 12, 269–274. <https://doi.org/10.1385/MB:12:3:269>

Lichty, J.J., Malecki, J.L., Agnew, H.D., Michelson-Horowitz, D.J., Tan, S., 2005. Comparison of affinity tags for protein purification. *Protein Expression Purif.* 41, 98–105. <https://doi.org/10.1016/j.pep.2005.01.019>

Malik, A., 2016. Protein fusion tags for efficient expression and purification of recombinant proteins in the periplasmic space of *E. coli*. *3 Biotech* 6, 44. <https://doi.org/10.1007/s13205-016-0397-7>

Mohammadian, H., Mahnam, K., Sadeghi, H., Ganjalikhany, M., Akbari, V., 2020. Rational design of a new mutant of tobacco etch virus protease in order to increase the *in vitro* solubility. *Res. Pharm. Sci.* 15, 164–173. <https://doi.org/10.4103/1735-5362.283816>

Nam, H., Hwang, B.J., Choi, D.-Y., Shin, S., Choi, M., 2020. Tobacco etch virus (TEV) protease with multiple mutations to improve solubility and reduce self-cleavage exhibits enhanced enzymatic activity. *FEBS Open Bio* 10, 619–626. <https://doi.org/10.1002/2211-5463.12828>

Plavša, J.J., Řezáčová, P., Kugler, M., Pachel, P., Brynda, J., Voburka, Z., Čelić, A., Petri, E.T., Škerlová, J., 2018. *In situ* proteolysis of an N-terminal His tag with thrombin improves the diffraction quality of human aldo-keto reductase 1C3 crystals. *Acta Crystallogr. Sect. F Struct. Biol. Cryst. Commun.* 74, 300–306. <https://doi.org/10.1107/s2053230x18005721>

Qi, R., Otting, G., 2019. Mutant T4 DNA polymerase for easy cloning and mutagenesis. PLoS One 14, e0211065. <https://doi.org/10.1371/journal.pone.0211065>

Raran-Kurussi, S., Tözsér, J., Cherry, S., Tropea, J.E., Waugh, D.S., 2013. Differential temperature dependence of tobacco etch virus and rhinovirus 3C proteases. Anal. Biochem. 436, 142–144. <https://doi.org/10.1016/j.ab.2013.01.031>

Raran-Kurussi, S., Waugh, D.S., 2012. The ability to enhance the solubility of its fusion partners is an intrinsic property of maltose-binding protein but their folding is either spontaneous or chaperone-mediated. PLOS One 7, e49589. <https://doi.org/10.1371/journal.pone.0049589>

Sanchez, M.I., Ting, A.Y., 2020. Directed evolution improves the catalytic efficiency of TEV protease. Nat. Methods 17, 167–174. <https://doi.org/10.1038/s41592-019-0665-7>

Tropea, J.E., Cherry, S., Waugh, D.S., 2009. Expression and purification of soluble His<sub>6</sub>-tagged TEV protease. Meth. Mol. Biol. 498, 297–307. <https://doi.org/10.1007/978-1-59745-196-3>

Ullah, R., Shah, M.A., Tufail, S., Ismat, F., Imran, M., Iqbal, M., Mirza, O., Rhaman, M., 2016. Activity of the human rhinovirus 3C protease studied in various buffers, additives and detergents solutions for recombinant protein production. PLOS One 11, e0153436. <https://doi.org/10.1371/journal.pone.0153436>

Walker, P.A., Leong, L.E.C., Ng, P.W.P., Tan, S.H., Waller, S., Murphy, D., Porter, A.G., 1994. Efficient and rapid affinity purification of proteins using recombinant fusion proteases. Nat. Biotechnol. 12, 601–605. <https://doi.org/10.1038/nbt0694-601>

Waugh, D.S., 2011. An overview of enzymatic reagents for the removal of affinity tags. Protein Expression Purif. 80, 283–293. <https://doi.org/10.1016/j.pep.2011.08.005>

Xu, H., Wang, Q., Zhang, Z., Yi, L., Ma, L., Zhai, C., 2019. A simplified method to remove fusion tags from a xylanase of *Bacillus* sp. HBP8 with HRV 3C protease. Enzyme Microb. Technol. 123, 15–20. <https://doi.org/10.1016/j.enzmictec.2019.01.004>

Yi, L., Gebhard, M.C., Li, Q., Taft, J.M., Georgiou, G., Iverson, B.L., 2013. Engineering of TEV protease variants by yeast ER sequestration screening (YESS) of combinatorial libraries. Proc. Natl. Acad. Sci. USA 110, 7229–7234. <https://doi.org/10.1073/pnas.1215994110>

Youell, J., Fordham, D., Firman, K., 2011. Production and single-step purification of EGFP and a biotinylated version of the human rhinovirus 14 3C protease. Protein Expression Purif. 79, 258–262. <https://doi.org/10.1016/j.pep.2011.05.003>

Zhang, Y., Olsen, D.R., Nguyen, K.B., Olson, P.S., Rhodes, E.T., Mascarenhas, D., 1998. Expression of eukaryotic proteins in soluble form in *Escherichia coli*. Protein Expression Purif. 12, 159–165. <https://doi.org/10.1006/prep.1997.0834>